Numerical study of optoelectromechanical effects in quantum dot arrays

Melnik, R.V.N., Lassen, B., Lew Yan Voon, L. and Willatzen, M.

In: Proceedings of the 17th IMACS World Congress on Scientific Computation, Applied Mathematics and Simulation, Eds. Borne P. et al, ISBN 2-915913-02-1, 6 pages, 2005.

Numerical Study of Optoelectromechanical Effects in Quantum Dot Arrays

R.V.N. Melnik[1], **B. Lassen, L.C. Lew Yan Voon, and M. Willatzen**

[1]Mathematical Modelling & Computational Sciences,
Wilfrid Laurier University, 75 University Ave W.,
Waterloo, ON, Canada N2L 3C5
Phone: +1-519884-1970(3662), Fax: +1-519-884-9738, E-mail: rmelnik@wlu.ca

[2]Mads Clausen Institute, Syddansk University,
Grundtvigs Alle 150, Sonderborg, DK-6400, Denmark

[3] Department of Physics, Wright State University,
3640 Colonel Glenn Highway, Dayton,
OH 45305, United States

Abstract - The paper focuses on a systematic construction of mathematical models for the analysis of low-dimensional semiconductor nanostructures, in particular quantum dots. We discuss nonlinear effects, including strain relaxation, as well as the piezoelectric effect that becomes increasingly important for the structures with hexagonal symmetry. 3D model reductions are also discussed and an example of such a reduction for cylindrical symmetry is given. Finally, representative examples of the results of numerical simulations are provided.

Keywords—**Quantum dots, Modelling, Coupled PDEs, Strain relaxation, Bandstructure calculation.**

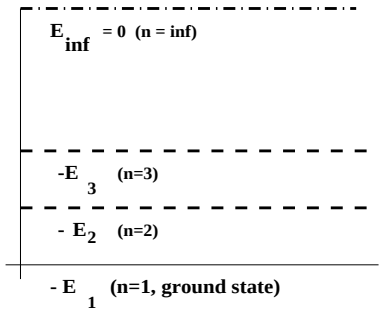

Fig. 1. A schematic electron energy level diagram.

I. INTRODUCTION

The bandstructures of semiconductors have been studied extensively at least from the late 50ies. By now, mathematical models for bandstructure calculation have achieved a certain degree of maturity. New technological advances in applications of low-dimensional semiconductor nanostructures (LDSN) led us to a situation where an accurate analysis of bandstructures requires the development of mathematical models that couple bandstrucrure calculation with the description of optoelectromechanical properties. It became clear that models based only on a linear Schrodinger model in the steady-state approximation may not be sufficient for modelling LDSN. Experiments (e.g., [ZAS 95]) provide a clear indication that a large spectrum of important effects may influence substantially on optoelectromechanical properties of the nanostructures, and among such effects is strain relaxation. Bonding of atoms to form molecules of matter occurs through the interaction of the valence electrons of each atom. Electrons have a dual nature and the values of electron energies are represented by energy level diagrams as depicted schematically in Fig. 1. The energy levels of individual atoms in solids form bonds of energies and electrical properties are then determined by the valence and conduction bands and by a gap or the forbidden band. The ability of (valence) electrons to bridge this gap and to move into the conduction band determines whether the solid is a conductor, a semiconductor, or an insulator. In semiconductors the valence electrons have sufficient energy to bridge the gap and become free electrons in the conduction band.

While in pure (or intrinsic) solids we simply have a balance between the electrons in the conduction band and electron vacancies (or holes) in the valence band, in most semiconductor applications we have to deal with a fairly complex dynamic process where electrons and holes (electron-hole pairs) continuously generate and recombinate. This process requires quite sophisticated mathematical models that would allow us to combine its continuous and discrete features.

In this paper, we review mathematical models for the description of electron-hole plasma of semiconductors and explain how such models can be supplemented by Schrodinger-type models for bandstructure calculation. Then, we discuss models obtained by averaging over atomic scales and couple such models with models for strain relaxation and piezoelectric effects. Nonlinearities induced by these effects are also discussed. Several representative examples based on the results of computational experiments are also given.

II. Mathematical models for semiconductors

In order to describe the process of interactions of electrons and holes, we start with the Liouville equation for the evolution of the position-velocity probability density $f(x, v, t)$:

$$\partial_t f + v \cdot \text{grad}_x f + 1/m\mathcal{F} \cdot \text{grad}_v f = 0, \tag{1}$$

$$t > 0,\ x \in \mathbb{R}^{3M},\ v \in \mathbb{R}^{3M},$$

$$f(x, v, t = 0) \geq 0,\ \int\int f(x, v, t = 0)dxdv = 1,$$

where, neglecting magnetic fields, we set

$$\mathcal{F} = -qE. \tag{2}$$

An idealized colissionless limit of this model leads to the Vlasov equation which, in the case when the effective field equation becomes the Poisson equation, can be reduced to a standard macroscopic conservation law:

$$q\partial_t n - \text{div}J = 0, \tag{3}$$

where $J = -q\int vFdv$ is the current density. For large-scale simulation this model is inadequate and has to be extented to account for the effect of collisions:

$$\partial_t F + v \cdot \text{grad}_x F + 1/m\mathcal{F}_{eff} \cdot \text{grad}_v F = Q(F). \tag{4}$$

In (4) $F(x, v, t)$ is the number density. In its essence, nonlinearities in this model are defined by the effective field model and by the model for collisions (e.g., [MAR 90]). Based on (4), a hierarchy of mathematical models can be constructed. The models in such a hierarchy can be classified according to the relationships between different relaxation times participating in the model, namely (a) the average time between two consecutive collisions, (b) the relaxation time of energy, and (c) the relaxation time of momentum. As discussed in [MEL 00b], many practically important cases would lead to the following quasi-hydrodynamic model:

$$\begin{cases} \partial_{xx}\varphi = q(n - p - N)/\epsilon\epsilon_0 \\ \partial_t n - \partial_t J_n/q = F, \\ \partial_t p + \partial_t J_p/q = F, \\ \partial_t \bar{\mathcal{E}}_n + \partial_x Q_n = -J_n\partial_x\varphi + P_n, \\ \partial_t \bar{\mathcal{E}}_p + \partial_x Q_p = J_p\partial_x\varphi + P_p, \end{cases} \tag{5}$$

where carrier current densities, J_n, J_p and flux energies, Q_n and Q_p are defined as follows

$$J_n = -qn\mu_n\partial_x\varphi + \partial_x(T_n\mu_n n), \tag{6}$$

$$J_p = -qp\mu_p\partial_x\varphi - \partial_x(T_p\mu_p p), \tag{7}$$

$$Q_n = \beta_n T_n n\mu_n\partial_x\varphi - \beta_n\partial_x[T_n D_n n]/q, \tag{8}$$

$$Q_p = -\beta_p T_p p\mu_p\partial_x\varphi - \beta_p\partial_x[T_p D_p p]/q. \tag{9}$$

This model has a convenient form for accounting for quantum effects. Indeed, the smooth quantum hydrodynamic approximation has the same form as above, but constitutive relations for the stress tensor, energy density, and the heat flux should incorporate now both classical and quantum effects. The approach described above offers a substantial speed up compared to classical Schrodinger's based models.

At a fundamental level, however, we will start from the mixed-state Schrodinger equation coupled to Poisson's equation for the electrostatic potential. Even such a simplified model is very difficult to deal with at a computational level due to its high dimensionality. Hence, in the next section we discuss how this model can be approximated in a consistent and efficient manner.

III. The process of QD formation and band structure calculation

In what follows, our focus will be on LDSN and in particular on quantum dots. Their formation is a result of competitive processes between the surface energy in the structure and strain energy. The end result of modern technologies for growing quantum dots is a structure with dozens and often hundreds self-assembled dots sitting on the wetting layer and distributed over it in a random-like non-uniform manner. The reality is fundamentally different from current models that use idealizations of isolated single quantum dots. Indeed, as observed on AFM images, quantum dots that are located on the substrate have different size and shape which lead to different optoelectromechanical properties. One of the effects that received a substantial attention in the literature is the effect of strain relaxation. Indeed, this effect becomes increasingly important for new applications of LDSNs ranging from life science to quantum computing.

As we have already pointed out, the general model discussed above is too complex to be used directly. Even the problem of calculating the full energy spectrum of a single symmetric quantum dot, including Coulomb interactions between charges and other effects, is difficult to solve. If we add to this the influence of the wetting layer [MEL 04] and piezoelectric effects, ab initio and atomistic methodologies become unpractical as ultimately we have to deal with an array of many individual quantum dots with several hundred thousand atoms each, sitting on the wetting layer. Although recent reports indicate that taken each quantum dot in isolation can be managed, accounting for the wetting layer [MEL 04] would increase the computational complexity substantially. It would be worthwhile also to note that for such large scale simulations, we still use an approximate Hamiltonian as the definitions of atomic forces are approximate. In this situation, it seems natural to seek

some averaging procedures over atomic scales. Among such procedures we shall mention methodologies based on empirical tight-binding, pseudopotential, and $k \cdot p$ approximations. The latter approach (the $k \cdot p$ theory) represents the electronic structure in a continuum-like manner, so it provides a convenient framework for including additional effects such as strain and piezoelectric effects.

Our examples that follow are related to wurtzite (WZ) semiconductors. These hexagonal WZ materials lead to a more challenging problem from a mathematical point of view compared to the materials with cubic symmetry. The bulk Hamiltonian with spin-orbit interaction in this case cannot be diagonalized at $k = 0$ if we use symmetry-adapted functions only. In these materials we have much more pronounced strain and piezoelectric effects as compared to cubic ZB materials.

The accuracy of the $k \cdot p$ (the envelope function) approximation depends on the choice of the functional space where the envelope function is considered. For WZ materials the standard Rashba-Sheka-Pikus Hamiltonian was adapted in [MIR 00] and was used recently in [FON 03]. Note in this context that when we use the six-band valence Hamiltonian for WZ materials, we will have to deal with 10 parameters compared to only 4 in the case of ZB materials. The basis functions, that span a space where the envelope function is sought, correspond to subbands within conduction and valence bands of the semiconductor material. The number of such basis functions is dictated by a balance between the accuracy of the model and computational feasibility of its solution. From a physical point of view, when studying optoelectronic properties of WZ materials we have to include spin-orbit and crystal-field splitting effects, as well as the effects of valence and conduction band mixing due to a large band gap typical for these materials. For the six valence subbands and 2 conduction subbands that count for spin up and down we have the following eigenvalue PDE problem

$$H\Psi = E\Psi, \tag{10}$$

$$\Psi = (\psi_S^{\uparrow}, \psi_X^{\uparrow}, \psi_Y^{\uparrow}, \psi_Z^{\uparrow}, \psi_S^{\downarrow}, \psi_X^{\downarrow}, \psi_Y^{\downarrow}, \psi_Z^{\downarrow})^T. \tag{11}$$

This problem should be solved with respect to eigenpair (Ψ, E), where $\psi_X^{\uparrow} \equiv (|X> \mid \uparrow)$ denotes the wave function component that corresponds to the X Bloch function of the valence band with the spin function of the missing electron "up", the subindex "S" denotes the wave function component of the conduction band, etc, and E is the electron/hole energy. Formally, the form of the Hamiltonian is the same for both, the standard Kohn-Luttinger Hamiltonian and its Burt-Foreman correction:

$$H \equiv -\frac{\hbar^2}{2m_0} \nabla_i \mathcal{H}_{ij}^{(\alpha,\beta)}(\vec{r}) \nabla_j, \tag{12}$$

representing the kinetic energy plus a nonuniform potential field and other effects contributing to the total potential energy of the system. The (α, β) indeces denote a basis for the wave function of the charge carriers. Problem (10) is determined by the 8×8 matrix Hamiltonian.

It is essential to account for strain effects in this model as atomic displacements collectively induce strain in our finite structure. This modifies the bandstructures and properties obtainable for idealized situations without accounting for strain effects become inadequate. Practically all current models for bandstructure calculations are based on the original representation of [BIR 74] where strain is treated on the basis of infinitesimal theory with Cauchy relationships between strain and displacements. However, geometric irregularities require improved approaches.

IV. Nonlinearities, coupling, and model reduction

In a standard manner, we define the result of the deformation $x_i \to \xi_i = x_i + u_i$ by the variation of deformation $\delta\epsilon_{ij}$. Then, since the LDSN is an initially stressed we take the second order approximation in the form of Eulerian components of the strain:

$$\epsilon_{ij} = \frac{1}{2}\left(\partial u_i/\partial x_j + \partial u_j/\partial x_i + \frac{\partial u_k}{\partial x_i}\frac{\partial u_k}{\partial x_j}\right). \tag{13}$$

This allows us to account for nonlinearities of geometric origin as strain inhomogeneities may substantially influence on the properties of the nanostructure.

In modeling LDSNs, we may need to account also for material nonlinearities, expressed by stress-strain relationships. Since strain remains of orders of magnitudes smaller of the elastic limits the linear relationship provides a good initial approximation. Note also that since semiconductors are piezoelectrics, higher order effects may become important at the level of device simulation. Another source of nonlinear effects is coming from the fact that elastic and dielectric coefficients, being functions of the structure geometry, are nonlinear, but the classical elasticity uses the valence-force field approaches. At the same time, at a fundamental level, the standard Keating model, that has parameters of unit-cell-dimension dependent, may not be sufficient. Strictly speaking, many body interactions of higher orders may need to be considered to account for anharmonicity effects and asymmetry of the interatomic potential.

Another important effect in semiconductors with hexagonal symmetry is the piezoelectric effect which may substantially contribute to bandstructures. This effect is incorporated into the model via equilibrium equations:

$$\frac{\partial \sigma_{ij}}{\partial x_j} + \rho F_i(\xi_l) = 0, \tag{14}$$

supplemented by appropriate boundary conditions. In this context, we note that for our experiments we assume that

the LDSN is embeded in a larger matrix material where Dirichlet boundary conditions for displacements are assumed. The coupling between mechanical and thermal fields for hexagonal WZ materials is determined by the constitutive equations:

$$\begin{aligned}
\sigma_{xx} &= c_{11}\epsilon_{xx} + c_{12}\epsilon_{yy} + c_{13}\epsilon_{zz} - e_{13}E_z,\\
\sigma_{yy} &= c_{12}\epsilon_{xx} + c_{11}\epsilon_{yy} + c_{13}\epsilon_{zz} - e_{31}E_z,\\
\sigma_{zz} &= c_{13}(\epsilon_{xx} + \epsilon_{yy}) + c_{33}\epsilon_{zz} - e_{33}E_z,\\
\sigma_{yz} &= c_{44}\epsilon_{yz} - e_{15}E_y,\\
\sigma_{zx} &= c_{44}\epsilon_{zx} - e_{15}E_x,\\
\sigma_{xy} &= \frac{1}{2}(c_{11} - c_{12})\epsilon_{xy}.
\end{aligned}$$

System (14) is solved together with the Maxwell equation for the piezoelectric potential:

$$\nabla \cdot \mathbf{D}(r) = 0, \tag{15}$$

where $\mathbf{D}$ is the vector of electric displacement and the remaining triplet of constitutive equations has the form:

$$\begin{aligned}
D_x &= e_{15}\epsilon_{zx} + \varepsilon_{11}E_x, \quad D_y = e_{15}\epsilon_{yz} + \varepsilon_{11}E_y,\\
D_z &= e_{31}(\epsilon_{xx} + \epsilon_{yy}) + e_{33}\epsilon_{zz} + \varepsilon_{33}E_z + P_{sp},
\end{aligned}$$

where P_{sp} is the spontaneous polarization, and $\mathbf{E} = -\nabla\varphi$. In some cases 3D bandstructure calculation models are amenable to dimensional reductions (e.g., [WIL 04], [VOO 04]), but in the general case the presence of essentially 3D physical effects such anisotropy, polarization, as well as of geometric inhomogeneities, complicates substantially such reduction procedures.

V. Weak formulation and Hamiltonian approximation

The above problem is reformulated in the variational form and is coupled to the weak form of the Schrodinger equation. The latter, as was pointed out in [JOH 03], is equivalent to finding stationarity conditions for the following functional:

$$-\frac{\hbar^2}{2m_0}\int_{\tilde{V}} (\nabla\Psi)^T \mathcal{H}^{(\alpha,\beta)} \nabla\Psi dv - E\int_{\tilde{V}} \Psi^T\Psi dv \tag{16}$$

with respect to the wave function vector field Ψ defined in (10).

We complete the formulation of the problem by specifications for Hamiltonian approximation. Our Hamiltonian is formally represented as a sum of constant and k-dependent energies:

$$H = H_0 + \tilde{\mathcal{H}}, \quad \tilde{\mathcal{H}} = H_1 + H_2 + H_3, \tag{17}$$

where H_0 (which is usually derived from the standard Kane Hamiltonian at $k = 0$) accounts for the spin-splitting effects. The corresponding spin-orbit coupling matrix for the WZ materials can be found, for example, in [MIR 00], [FON 03]. The associated (with $k = 0$) matrix elements for the conduction band in (14) are zero. The second term, $\tilde{\mathcal{H}}$, consists of contributions of (a) the kinetic part of the microscopic Hamiltonian unit cell averaged by the respective Bloch function (S, X, Y, or Z), denoted as H_1, (b) the strain-dependent part of the Hamiltonian, denoted as H_2, and (c) the energy of unstrained conduction/valence band edges, denoted as H_3. For the conduction band, components of H_2 (the first and the fifth rows in the total Hamiltonian) are given as (e.g., [FON 03])

$$H_2^c(\vec{r}) = a_1\epsilon_{zz} + a_2(\epsilon_{xx} + \epsilon_{yy}) \tag{18}$$

with the conduction band deformation potentials a_1 and a_2 (coordinate dependent, but constants within each material), while for the valence bands (the 2nd, 3rd, and 4th rows, respectively) we have:

$$H_2^v(\vec{r}) = (hv_{ij}), \quad i,j = 1,2,3 \tag{19}$$

$$\begin{aligned}
hv_{11} &= l_1\varepsilon_{xx} + m_1\varepsilon_{yy} + m_2\varepsilon_{zz}\\
hv_{12} &= n_1\varepsilon_{xy}\\
hv_{13} &= n_2\varepsilon_{xz}\\
hv_{21} &= n_1\varepsilon_{xy}\\
hv_{22} &= m_1\varepsilon_{xx} + l_1\varepsilon_{yy} + m_2\varepsilon_{zz}\\
hv_{23} &= n_2\varepsilon_{yz}\\
hv_{31} &= n_2\varepsilon_{xz}\\
hv_{32} &= n_2\varepsilon_{yz}\\
hv_{33} &= m_3(\varepsilon_{xx} + \varepsilon_{yy}) + l_2\varepsilon_{zz}.
\end{aligned}$$

The above representation is given in the standard $(|X>, |Y>, |Z>)$ basis and the same expressions hold for the 6th, 7th, and 8th rows of our 8×8 Hamiltonian.

Finally, components of H_3 have diagonal entries of $-e\phi(\vec{r})$ where ϕ is the piezoelectric potential and e is the absolute value of the electron charge. H_1 has the standard form and for WZ materials and its components contain quadratic terms, related to the first order differential operators, in such a way that the resulting system of 8 partial differential equations is of elliptic type.

VI. Simplifications and model implementation

In the case of cylindrical symmetry, the general Hamiltonian for WZ structures, containing 10 parameters, can be reduced to a simpler form. This can be done by applying the Sercel-Vahala (SV) approach to the Rashba-Sheka-Pikus strain Hamiltonian (given for WZ structures, e.g., in

[MIR 00], [FON 03]). The result is an extention of what has recently been reported in [VOO 04] to the hexagonal WZ materials (given in the SV basis):

$$H = (h_{ij}), \quad i,j = 1,2,3, \tag{20}$$

$$\begin{aligned}
h_{11} &= S_{11} + \Delta_1 + \Delta_2 + S^{\varepsilon}_{11} \\
h_{12} &= S_{12} + S^{\varepsilon}_{12} \\
h_{13} &= S_{13} + S^{\varepsilon}_{13} \\
h_{21} &= S_{21} + S^{\varepsilon *}_{12} \\
h_{22} &= S_{22} + \Delta_1 - \Delta_2 + S^{\varepsilon}_{22} \\
h_{23} &= S_{23} + S^{\varepsilon}_{23} \\
h_{31} &= S_{31} + S^{\varepsilon}_{13} \\
h_{32} &= S_{32} + S^{\varepsilon}_{23} \\
h_{33} &= S_{33} + S^{\varepsilon}_{33},
\end{aligned} \tag{21}$$

where entries of strain terms are denoted by the superindex "ϵ". (only the 2nd, 3rd, and 4th rows are given; $h_{26} = h_{35} = \Delta$ and the rest of elements in these rows are zero; Rows 6,7, and 8 have analogous form).

Operators S_{ij} are second order differential operators obtained in a way similar to that described in [VOO 04], for example

$$\begin{aligned}
S_{22} = -\frac{\hbar^2}{2m_0}\frac{1}{2}\Bigg\{ &\frac{\partial}{\partial\rho}\left((L_1+M_1)\frac{\partial}{\partial\rho}\right) + \\
&\frac{(L_1+M_1)}{\rho}\frac{\partial}{\partial\rho} + \\
&2\frac{\partial}{\partial z}M_2\frac{\partial}{\partial z} + \frac{(F_z-J_2)}{\rho}\frac{\partial}{\partial\rho}(N_1-N_1') - \\
&\frac{(F_z-J_2)^2}{\rho^2}(L_1+M_1)\Bigg\}.
\end{aligned} \tag{22}$$

Based on such a reduced Hamiltonian it is convenient to model rods, cylindrical nanowires and superlattices.

Implementation of the formulated model is based on the three main steps.

Step 1. In order to compute optical spectra of quantum dot arrays, first we reduce the Maxwell equation to

$$\nabla(\epsilon\nabla\varphi) = -\rho + \nabla\cdot(P^s + P^p) \tag{23}$$

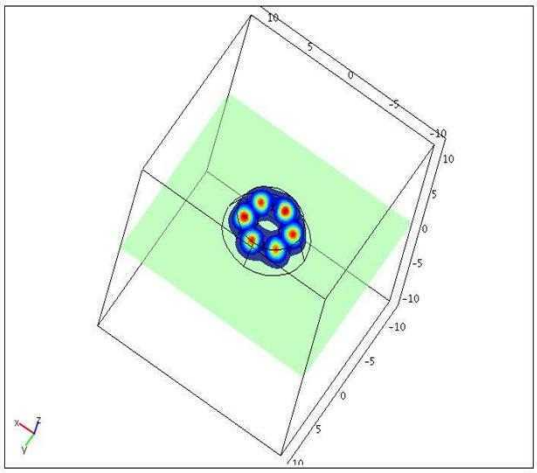

Fig. 2. Quantum dot eigenstate that corresponds to the sixth eigenvalue: the single dot case.

and solve it with the equilibrium equations:

$$\frac{\sigma_{xx}}{\partial x} + \frac{\partial\sigma_{xy}}{\partial y} + \frac{\partial\sigma_{xz}}{\partial z} = 0, \tag{24}$$

$$\frac{\sigma_{xy}}{\partial x} + \frac{\partial\sigma_{yy}}{\partial y} + \frac{\partial\sigma_{yz}}{\partial z} = 0, \tag{25}$$

$$\frac{\sigma_{xz}}{\partial x} + \frac{\partial\sigma_{yz}}{\partial y} + \frac{\partial\sigma_{zz}}{\partial z} = 0. \tag{26}$$

These equations are coupled by constitutive equations written for WX hexagonal materials. In the above equations P^s and P^p are spontaneous and strain-induced polarization, respectively.

Step 2. The outputs from this model allow us to define the Hamiltonian of system (2) on the same computational grid.

Step 3. By solving the remaining eight coupled elliptic PDEs (1), we find both eigenfunctions and energies corresponding to all subbands under consideration.

A few representative examples of computations with this model are demonstrated in Fig. 1–4. In Fig. 1 we present the 6th eigenvalue of a single quantum dot structure. In Fig. 2–4 we present the y-component of the displacement, strain component ϵ_x, and the electrostatic potential. In the latter case, all computations were carried out for a five dot array based on the WZ material.

REFERENCES

[ZAS 95] ZASLAVSKY, A. et al, Strain relaxation in silicon-germanium microstructures observed by resonant tunneling spectroscopy, vol.67, 3921, Appl. Phys. Let., 1995.

[MAR 90] MARKOWICH, P.A., RINGHOFER, C.A., and SCHMEISER, C., Semiconductor Equations, Springer-Verlag, 1990.

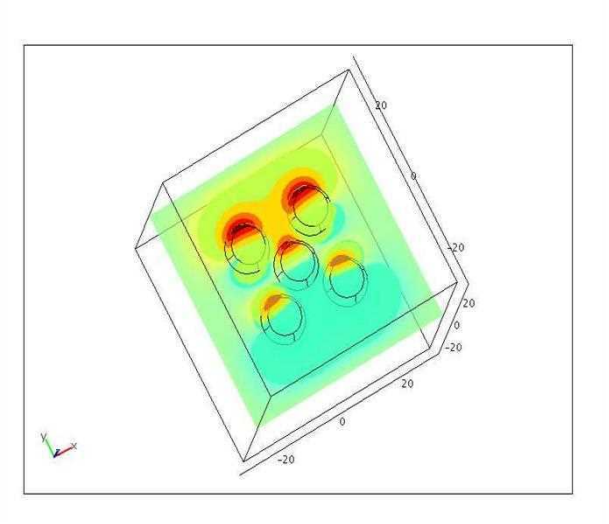

Fig. 3. The y-component of the displacement: the five-dot quantum molecule.

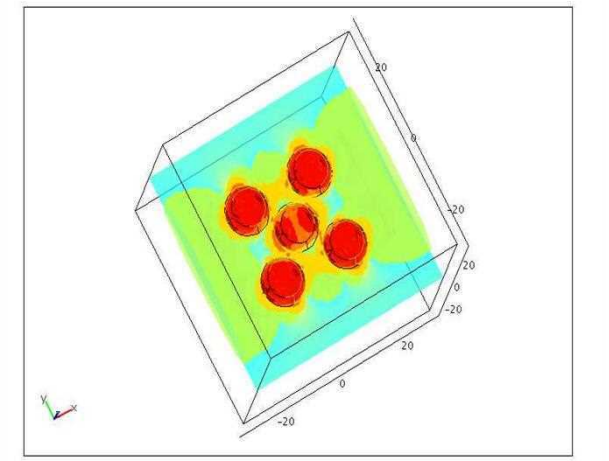

Fig. 4. The x-component of the strain: the five-dot quantum molecule.

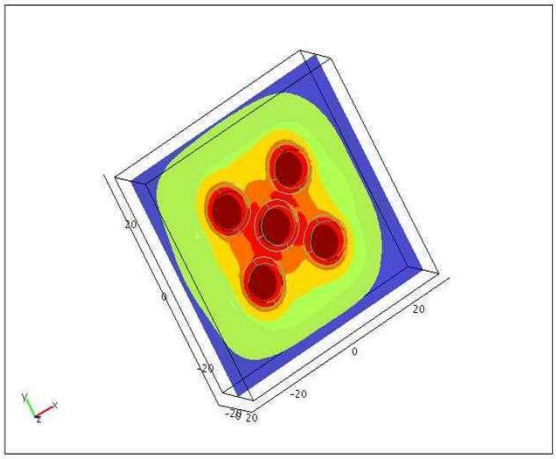

Fig. 5. Potential distribution in the the five-dot quantum molecule.

[MEL 00b] MELNIK, R.V.N. and HE, H., Modelling nonlocal processes in semiconductor devices with exponential difference schemes, vol. 38, p. 233–263, J. of Eng. Mathematics, 2000.

[MEL 04] MELNIK, R.V.N. and WILLATZEN, M., Bandstructures of conical quantum dots with wetting layers, vol. 15, p. 1–8, Nanotechnology, 2004.

[MIR 00] MIRELES, F. and ULLOA, S.E., Strain and crystallographic orientation effects on the valence subbands of wirtzite quantum wells, vol. 62, p. 2562–2572, Phys. Rev. B, 2000.

[FON 03] FONOBEROV, V.A., BALANDIN, A.A., Electronic properties of strained wurtzite and zinc-blende $GaN/Al_xGa_{1-x}N$ quantum dots, vol.94, p. 7178–7186, J. Appl. Phys., 2003.

[BIR 74] BIR, G.L. and PIKUS, G.E., Symmetry and Strain-Induced Effects in Semiconductors, John Wiley and Sons, N.Y., 1974.

[WIL 04] WILLATZEN, M., MELNIK, R.V.N., C. GALERIU, LEW YAN VOON, L.C., Quantum confinement phenomena in nanowire superlattice structures, vol. 65, p. 385–397, Mathematics and Computers in Simulation, 2004.

[VOO 04] LEW YAN VOON, L.C., MELNIK R., LASSEN, B., and WILLATZEN, M., Influence of aspect ratio on the lowest states of quantum rods, vol.4, p. 289–292, Nano Letters, 2004.

[JOH 03] JOHNSON, H.T. and BOSE, R., Nonoindentation effect on the optical properties of self-assembled quantum dots, vol.51, p. 2085–2104, J. Mech. Phys. Solids, 2003.

Honorary Chair:
Prof. Robert Vichnevetsky, Rutgers University - USA

General Chair:
Prof. Pierre Borne, Ecole Centrale de Lille - France

International Program Committee Chair:
Prof. Mohamed Benrejeb, ENIT - Tunisia
Prof. Spyros Tzafestas, NTUA - Greece
Prof. Serge Petiton, LIFL/INRIA - France

ECOLE CENTRALE DE LILLE
Cité Scientifique - BP 48
59651 Villeneuve d'Ascq Cedex - France
Phone: (33/0)3 20 33 53 53
Fax: (33/0)3 20 33 54 99
http://imacs2005.ec-lille.fr

ISBN: 2-915913-02-1
EAN: 9782915913026

Edited by:
Pierre Borne
Mohamed Benrejeb
Nathalie Dangoumau
Lionel Lorimier

17th IMACS World Congress

Scientific Computation, Applied Mathematics and Simulation

http://imacs2005.ec-lille.fr

Paris, France / July 11 - 15, 2005

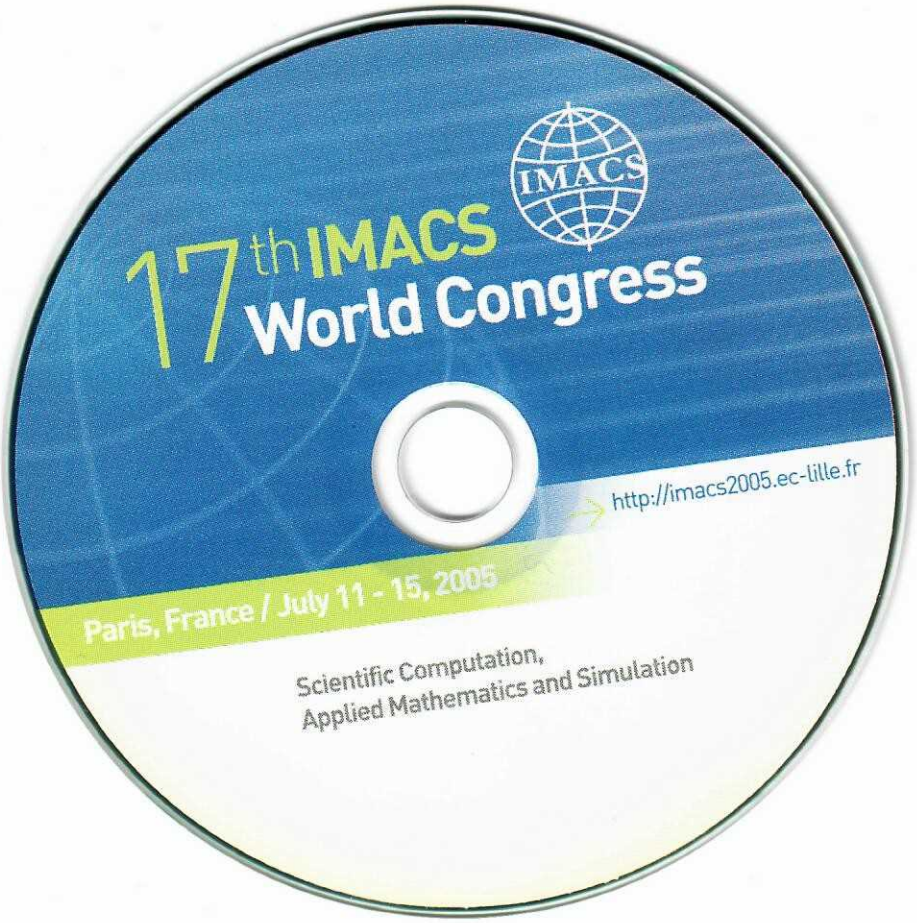
IMACS
17th IMACS
World Congress
http://imacs2005.ec-lille.fr
Paris, France / July 11 - 15, 2005
Scientific Computation,
Applied Mathematics and Simulation